Modeling the impacts of future LULC and climate change on runoff and sediment yield in a strategic basin in the Caatinga/Atlantic forest ecotone of Brazil

José Yure Gomes dos Santos[1], Suzana Maria Gico Lima Montenegro[2], Richarde Marques da Silva[3], Celso Augusto Guimarães Santos[4*], Nevil Wyndham Quinn[5], Ana Paula Xavier Dantas[4] and Alfredo Ribeiro Neto[2]

[1]Federal University of Rio Grande do Norte, Department of Geography, Caicó, Brazil

[2]Federal University of Pernambuco, Department of Civil Engineering, Recife, Brazil

[3]Federal University of Paraíba, Department of Geosciences, João Pessoa, Brazil

[4]Federal University of Paraíba, Department of Civil and Environmental Engineering, 58051-900 João Pessoa, Brazil

[5]Department of Geography and Environmental Management, University of the West of England, Bristol, UK

[*]*Corresponding author: celso@ct.ufpb.br*

Abstract:

Water management in the Caatinga/Atlantic forest ecotone in Brazil is critically dependent on better understanding of potential future changes in streamflow and sediment dynamics. This paper evaluates both the future impacts of land use and land cover (LULC) changes and the impacts of climate change on the streamflow and sediment yield in the Tapacurá River basin in northeastern Brazil, using a novel combination of approaches. Projected climate data derived using global circulation model HadGEM2-ES were coupled to regional circulation model ETA-CPTEC/HadCM3 for two representative concentration pathways (RCP 4.5 and 8.5), with bias correction. Two future LULC scenarios were generated: (a) optimistic (current LULC), and (b) pessimistic (land use change trends continue), using the multilayer perceptron algorithm (MP). The Soil and Water Assessment Tool (SWAT) model was used to estimate

future streamflow and erosion for different periods (2011−2040, 2041−2070 and 2071−2099). The SWAT model was calibrated for period 1995–2003 and validated for 2004–2013. The results showed good accuracy in relation to R^2, NSE and PBIAS for the calibration and validation of the runoff, as well as for the verification of the sediment yield. Simulations indicated significant increases in erosion for the pessimistic scenario under RCP 8.5, followed by the pessimistic scenario and RCP 4.5. Lower sediment yields occurred for the optimistic and RCP 8.5, with lower still for the optimistic and RCP 4.5. However, the latter estimates are still considerably higher than baseline conditions. Although higher flows are found for some scenarios, the increases in sediment yield have serious implications for reservoir siltation and storage reduction. Despite modeling uncertainty, the results demonstrate that the proposed methodology has promising scope to contextualize potentially significant regional hydrological changes which have implications for land and biodiversity management and the sustainability of water resources in the Caatinga/Atlantic forest ecotone.

Keywords: Streamflow; erosion; future scenarios; degradation; hydrologic modeling.

1. Introduction

Climate variation and climate change over the longer term, together with human activities, are the main factors that influence streamflow and erosion in catchments (Shi et al. 2013; Petelet-Giraud et al., 2017; Dai et al., 2020). Global climate change is widely acknowledged (de Oliveira et al., 2018), and many studies address the increasing concentration of greenhouse gases and associated changes in climate drivers and patterns (Liu et al., 2020; Marin et al., 2020; An et al., 2020). The increase in extreme hydrological events, for example, has caused environmental problems worldwide (Kusangaya et al., 2018; Zhao et al., 2020; Zhang et al., 2020; Wang et al., 2020; Santos et al., 2021; Brito et al., 2021), with direct impacts to the global economy and the lives of much of the population (Eamen et al., 2020). These include

increased floods and droughts, pollution of water resources, soil erosion, silting, and a reduction in the productive capacity of soils. This study represents the first application of modeling to assess the impacts of future LULC and climate change on runoff and sediment yield at a monthly scale in the ecologically important Caatinga/Atlantic forest ecotone of northeastern Brazil. Investigating the relative significance of LULC and climate change as drivers is of fundamental importance in understanding runoff and sediment yield behavior. Understanding the effects of LULC and climate change on sediment yield and streamflow in basins is a major challenge in contemporary water resource management (Cunha et al., 2020). The Caatinga/Atlantic forest ecotone area in northeastern Brazil, also known as "Agreste", is an internationally significant biodiversity hotspot, and critical in the regional water supply. The region is under-studied and a better understanding of future hydrological conditions is an urgent need (Da Silva et al., 2012).

Natural changes usually occur on scales of decades, whereas anthropogenic influences have the power to change hydrological dynamics in a short time (Bhatta et al., 2019). In particular, two human actions that result in LULC changes can be highlighted, deforestation, and the replacement of other native vegetation by agriculture, urban areas or other forms of occupation, which do not always provide as good protection of the soil against rainfall effects (Ursulino et al., 2019).

These changes are felt more strongly in transition regions such as the Caatinga/Atlantic ecotone forest. The Caatinga biome, also known as Dry Forest (Souza et al., 2019) is ecologically fragile and particularly sensitive to climate change, due to recurrent droughts (Correia et al., 2020). The adjacent Atlantic forest biome, home to a large part of the Brazilian population, has also been impacted by droughts and floods (Alvalá et al., 2019). Consequently, areas such as the Caatinga/Atlantic forest ecotone, require special efforts to preserve their important water resources and unique environment. The area is an international

77 biodiversity hotspot, and much of its biological heritage cannot be found elsewhere on the
78 planet (Da Rocha et al., 2020). The population and the economic activities within this biome
79 depend on its water resources, which are used mainly for irrigation and public supply, making
80 the population susceptible to climate variability as extreme events of flood and droughts
81 (Silva et al., 2020).

82 Hydrological models have previously been used to predict water resources under
83 projected warming in northeastern Brazil (Dos Santos et al., 2014; Silva et al., 2018; de
84 Andrade et al., 2019; de Medeiros et al., 2019). Recently, SWAT applications have been used
85 to analyze hydrologic behavior in basins of different scales (e.g., Čerkasova et al., 2018; Chen
86 et al., 2019; Marin et al., 2020), based on the coupling of hydrological and global circulation
87 models (GCM) (Braga et al., 2013). However, no studies have assessed runoff-erosion
88 dynamics using distributed hydrological models and LULC change estimation algorithms
89 coupled with bias corrected global and regional models for the Caatinga/Atlantic Forest
90 ecotone region. This study aims to address this need by providing an analysis of the combined
91 impacts of both potential climate and LULC changes, in support of developing urgent
92 strategic land, biodiversity and water management plans, including control approaches
93 (Montenegro and Ragab, 2012). In this study, the SWAT hydrological model driven by
94 climate simulations, estimated streamflow and annual sediment yield in a strategic basin of
95 northeastern Brazil (Tapacurá River basin), in response to climate change across three periods
96 (2011–2040, 2041–2070 and 2071–2099) using GCM data for two different gas emission
97 scenarios.

98

99 **2. Material and methods**

100 **2.1. Study area and methodological overview**

The Tapacurá River basin (470 km²) is situated in a transition area between the Caatinga and Atlantic forest biomes, in Pernambuco State, northeastern Brazil (Figure 1). The rainy season is from March to August and the annual rainfall ranges from 800 to 1,800 mm. The basin is classified as type As (equatorial, hot, and summer dry) in the Köppen-Geiger climate classification, with an annual average temperature of 27°C (da Silva et al. 2012).

The Tapacurá River basin is a significant water resource supply unit for the Recife Metropolitan Region (RMR), one of the largest population centers in Brazil, with approximately 3.7 million inhabitants (IBGE, 2020). The region has faced dry periods such as the drought of 1998, as well as periods of flooding, which were frequent until the 1970s. These extreme events have had numerous social, economic and environmental impacts and structural interventions have been required to minimize the effects of flooding in Recife city, the capital of the State.

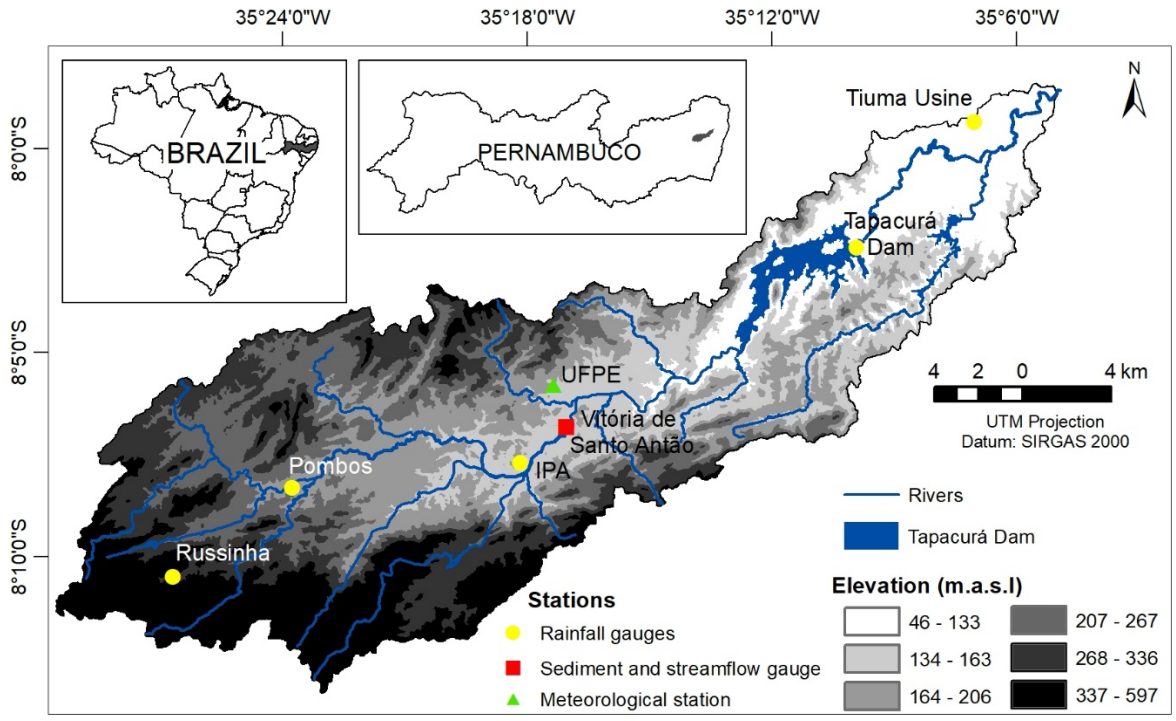

Figure 1. Location map of the Tapacurá River basin in Pernambuco state (Brazil).

The main reservoir is the Tapacurá Reservoir, was built in 1973 to supply about 40% of the RMR with water, and to control the periodic floods referred to above. The reservoir has a storage capacity of 95×10^6 m³, a maximum water surface of 9.7 km² (da Silva et al., 2012), and supplies water to approximately 1 million inhabitants of the RMR (Gunkel et al., 2003). The Tapacurá River basin is consequently a critical strategic water supply area for Pernambuco State, and hydrological processes in the basin have far-reaching implications for the RMR. This study therefore focuses specifically on the combined effects of projected climate change and LULC change on the runoff and sediment yield within the Tapacurá River basin.

Figure 2 provides a schematic of the research methodology. The SWAT model was calibrated and validated for the baseline period (1995-2012) using 2007 LULC. Landsat 5 imagery and an ANN algorithm was used to classify and map LULC change over time (1987-2015), generating a transition probability matrix. Following testing of the transition probabilities against observed LULC, LULC scenarios were generated for several future periods based on two sets of assumption (optimistic, pessimistic). A GCM was downscaled and corrected for two RCPs (4.5, 8.5), and used together with the LULC scenarios to estimate future streamflow and sediment yields.

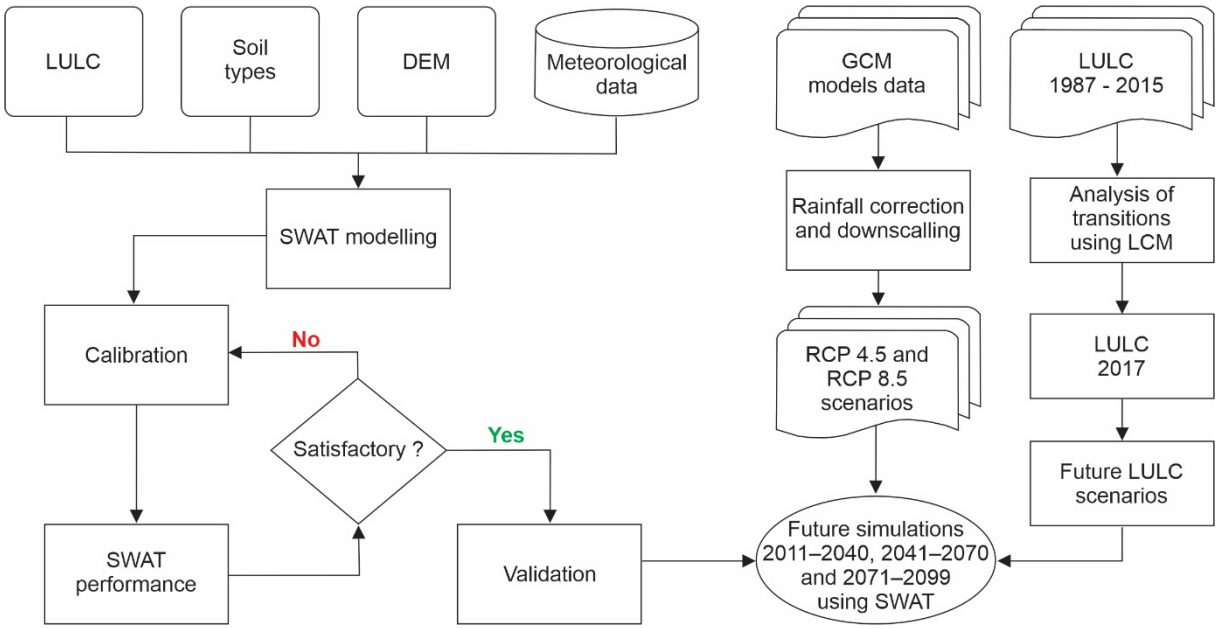

Figure 2. Schematic of the research methodology.

2.2. Data description

2.2.1. Rainfall and streamflow datasets

The observed daily rainfall and streamflow data were acquired from the Agência Nacional de Águas e Saneamento Básico (National Water and Sanitation Agency – NWSA), for five rain gauges, one weather station and a streamflow gauge within the study area (Figure 1). The observed daily streamflow data were acquired from Vitória de Santo Antão streamflow gauge for January 1995 to December 2012 (baseline), which were utilized for calibration (1995–2003) and validation (2004–2013) of the SWAT model.

2.2.2. DEM, soil type and LULC datasets

The digital elevation model (DEM) underpinning this work (Figure 3a) was derived from the 30m SRTM product (available at https://earthexplorer.usgs.gov). Three Landsat 5 images were utilized in mapping current LULC and developing future LULC scenario maps. These were from orbit 214 and point 66 for time periods t_1 (July 1987), t_2 (August 2007), and t_3

(July 2015). These images were chosen because they represent an interval considered suitable for analyzing changes in the LULC. The LULC map (Figure 3b), used as an input for the baseline SWAT modeling was generated through the classification of the t_2 image (2007). Seven LULC classes were identified, namely, agriculture, livestock, sugarcane, rain forest, urban areas, water and Caatinga vegetation. According Ragab et al. (2012), the Tapacurá River basin is characterized by deforestation, with most of the original rain forest having been cleared during the last decades (1980–2010). Caatinga, a vegetation type similar to Savanna and typical of northeastern Brazil, remains, but a large area of the basin is now occupied by farmlands and sugar cane production (Montenegro and Ragab, 2012). The soil map was derived from the EMBRAPA (1999) at a scale of 1:100,000. The soil types within the basin are acrisols, gleysols, ferralsols, chromic luvisols, fluvisols, leptosols, regosols and planosols (Figure 3c). Figure 3d shows slopes of the basin.

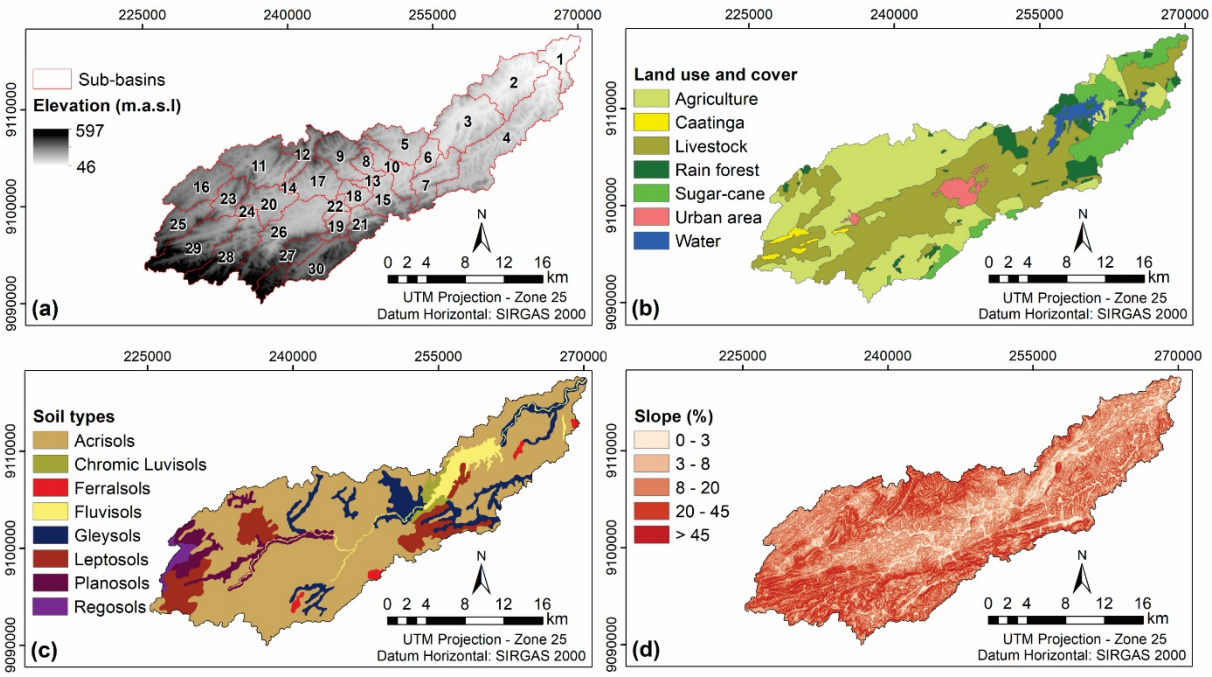

Figure 3. (a) DEM and sub-basins, (b) LULC in 2007, (c) soil types, and (d) slopes of Tapacurá River basin.

2.3 Evaluation of classification

In order to determine the accuracy of the classification process, classified images with land use data that were derived from ground-truth data, were used. These data are assumed to be a 'true' representation of land use. In this study, evaluating the accuracy of the classification was accomplished by applying thresholding and accuracy assessment methods, such as kappa statistics, omission and commission errors. Omission error estimates the probability of a pixel being accurately classified. This is the result from dividing the number of correctly classified pixels in each LULC class by the number of training pixels determined from the ground-truthed data. This reveals how well training set pixels of the given LULC type are classified. Commission error shows the probability that a pixel represents the class for which it has been assigned. This is computed by dividing the number of correctly classified pixels in each category by the total number of pixels in that category. The relationship between these two sets of information (classified pixels and commission error) is usually summarized in an error matrix, also named a confusion matrix. The number of rows and columns in the error matrix should be equal to the number of categories whose classification accuracy is being assessed (Lillesand and Kiefer, 2000). In the error matrix, the pixels located along the diagonal (from the upper left to the lower right) represent the pixels classified into the proper category. The non-diagonal values in the columns represent the omission error, while the non-diagonal values in the rows represent the commission error. The kappa statistic is used to measure the agreement between variables (McHugh, 2012). This index is a discrete multivariate measure of the actual concordance minus the concordance per chance (Cunha et al., 2021); i.e., it is a measure of the consistency between the classification and the reference data. The kappa statistic is calculated as:

$$\kappa = \frac{n\sum_{i=1}^{C} x_{ii} - \sum_{i=1}^{C} x_i + x +_i}{n^2 - \sum_{i=1}^{C} x_i + x +_i} \quad (1)$$

where x_{i+} is the sum of row i and x_{+i} is the sum of column i of the confusion matrix.

193

194 **2.4 LULC scenarios and validation of LULC prediction**

195 To quantify and map the changes of each LULC class, we used the land change modeler
196 (LCM) integrated into TerrSet software (Clark Labs, 2020) package. Two predicted LULC
197 scenarios were used to analyze the influence of future climate on streamflow and sediment
198 yield: (a) optimistic: current (2007) LULC conditions are maintained in the longer term
199 (Figure 3b), and (b) pessimistic: future changes in LULC (2050) considering intensification of
200 sugar cane monoculture, growth of urban areas and loss of rain forest and Caatinga
201 vegetation. For the creation of the pessimistic LULC map for 2050 (t_4), three Landsat 5
202 images from 1989 (t_1), 2007 (t_2), and 2015 (t_3) were analyzed using the multilayer perceptron
203 (MP) algorithm.

204 In this study, we overlay t_1, t_2, and a simulation map of t_3. LCM produces three types of
205 results (pixels): misses, hits, and false alarms. Predicting hits (changed) means the t_3 map
206 shows change and the simulation shows change. Predicting hits (not changed) or misses show
207 change, but the simulation shows persistence. False alarm means the t_3 map show persistence,
208 but the simulation shows change.

209 An estimate of LULC for 2015 was obtained by assessing the changes in area based on
210 t_1 and t_2 using the MP algorithm. The validation of LULC prediction was analyzed using the
211 kappa statistics. Then, this estimate of LULC for 2015 was compared with the observed
212 LULC (t_3) with kappa statistics of about 87%. The learning algorithm is considered to have
213 satisfactorily simulated the transition potential of LULC when the MP accuracy is greater
214 than or equal to 80%. Based on this result, the time t_3 (2015) was specified, and the ANN was
215 employed to determine the transition probability matrix from t_2 (2007) for t_3 (2015). See
216 Section 3.3 for how this was applied to estimate 2050 LULC.

The MP algorithm referred to above performed image classification by means of an artificial neural network (ANN) classifier using the back-propagation approach (Silva et al., 2020). As recommended by Ahmadlou et al. (2016), a configuration where 60% of the modified cells were used for MP training, with the remaining 40% retained for validation, was used. In this study, we used 15,000 iterations, because it was noted that the error curve decreased and stabilized at this number. In addition, the kappa statistics (Landis & Koch, 1977) were used to assess classification validity.

In order to validate the estimated LULC, and assess the performance of the LULC change probability, the total operating characteristics (TOC) approach (Pontius Jr. and Si, 2014) was used to evaluate the accuracy of the simulation. AUC is an area under a curve obtained using TOC method. An AUC value greater than the baseline value of equal to 0.5 indicates that the quality of the modeling results is satisfactory, whereas a value equal to 1 corresponds to a perfect fit (Chen et al., 2019). Additionally, the area under the curve (AUC) method was used to assess the result accuracy (Silva et al., 2020). These methods contemplate multiple thresholds and creates contingency tables that compare the performance of the probability of LULC changing. This approach is commonly used in studies of LULC change, urban growth and climate forecasting (Li and Chen, 2020).

2.5 Simulation accuracy and SWAT performance evaluation

The Soil and Water Assessment Tool (SWAT) model (Arnold et al. 1998) is a comprehensive, semi-distributed multi-parameter hydrologic model and is one of the most used models for modeling runoff and sediment yield (Silva et al., 2018). The Sequential Uncertainty Fitting procedure (SUFI-2) (Abbaspour et al., 2007) within the SWAT Calibration Uncertainty Procedures (SWAT-CUP) tool, was used to calibrate monthly streamflow based on data from the Vitória de Santo Antão streamflow gauge. A Split Sample Test was applied, i.e. three

years were considered for warm-up (1992–1994), nine years for calibration (1995–2003) and nine years for validation (2004–2012).

Tapacurá River basin is an ungauged basin for sediment data, which are measured only during random campaigns. The SWAT model was calibrated for estimation of sediment yield using a sediment-discharge rating curve. The sediment load is given by the rating curve (Equation 2 and Figure 4) for the Vitória de Santo Antão streamflow gauge, based on field measurements.

$$S_y = 6.1496Q^{1.6399} \quad (2)$$

where S_y is the sediment yield (mg/day) and Q is the streamflow (m^3/s).

The mean daily *in-situ* suspended sediment curve equals the ratio between the sediment load and the river discharge. The sampling of suspended sediments is performed by the Geological Survey of Brazil using isokinetic samplers by vertical integration and the sampling method by equal width increment (EWI), as described in Carvalho (2008). This station falls within the responsibility of NWSA and has observed sediment data from 1995 to 2012 obtained on an irregular basis over a period of years by the Geological Survey of Brazil.

Over the simulation period, sediment data were obtained on 8 days. The small number of measurements is due to the fact that the Geological Survey of Brazil schedules visits to monitoring cross-sections annually (three visits) and is not always able to carry out the scheduled collections due to river conditions. The sediment station is located in a river that is within an urban area, and after intense rainfall events, runoff produces very strong currents which prevent measurement.

This approach has been used because sediment-discharge rating curves have been successfully applied in other basins with limited sediment data (dos Santos et al., 2015). The results of the streamflow and sediment yield simulations were calibrated to maximize the R^2, Nash–Sutcliffe efficiency (NSE) and relative bias (PBIAS), based on Moriasi et al. (2007).

267 Moreover, two tests have been applied for evaluation of model performance and uncertainty,
268 i.e., p-factor (observations bracketed by the prediction uncertainty) and the r-factor
269 (achievement of small uncertainty band).

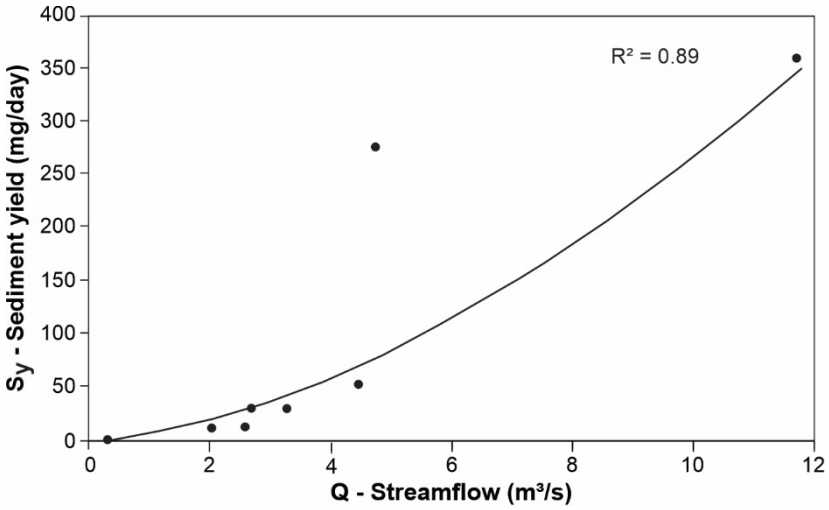

270

271 **Figure 4.** Sediment rating curve for the Vitória de Santo Antão sediment gauge.

272

273 **2.6 Future climate projections and bias correction**

274 To provide long-term simulations of future climate at a suitable spatial resolution, a regional
275 climate circulation ETA-CPTEC/HadCM3 model (Chou et al., 2014a; Chou et al., 2014b) was
276 coupled with a GCM (Hadley Centre Global Environmental Model version 2 - HadGEM2-
277 ES) (Collins et al., 2011). Within the Coupled Model Intercomparison Project (Van Vuuren et
278 al., 2011; Nilawar and Waikar, 2019), the IPCC defines several scenarios for future climate
279 projection named representative concentration pathways (RCPs). For example, RCP 2.6
280 means the radiative forcing level reaches 3.1 W/m^2 by mid-century but returns to 2.6 W/m^2 by
281 2100, with low driving levels of greenhouse gas emissions. RCP 4.5 considers carbon
282 emissions to reach around 650 ppm, and RCP 8.5 has high greenhouse gas emissions (around
283 1370 ppm).

284 In this study, RCP 4.5 and RCP 8.5 were used for the periods of 2011–2040, 2041–
285 2070 and 2071–2099. Currently GCMs data have excellent results on medium and large

286 basins, however they may contain systematic error so cannot be downscaled and used as
287 model inputs without bias correction (Tapiador et al. 2020). In our work, a linear scaling
288 approach is applied to improve the GCMs rainfall data.

289 The ETA-CPTEC/HadCM3 data showed bias for the rainfall and air temperature
290 variables, which are generally underestimated when compared with the observed values.
291 Corrections for systematic errors (bias correction) in the ETA-CPTEC/HadCM3 modeled
292 future precipitation were made using cumulative distribution functions (CDFs) for both
293 variables, as proposed by Bárdossy and Pegram (2011), and used by Berg et al. (2012) and
294 Ribeiro Neto et al. (2014). In this study, we used observed data from 1961 to 1990. The mean
295 bias was inserted into the model data after calculating the bias for each month of the
296 climatological year.

297

298 **3. Results**

299 **3.1 Sensitivity of SWAT parameters**

300 The first step in the model calibration and validation process is the determination of the most
301 sensitive parameters in the modeling. In this study, 19 parameters that influence the
302 streamflow were identified and a sensitivity analysis of all SWAT model parameters was
303 obtained after 500 iterations using the SWAT-CUP calibration procedure. Ten of these were
304 identified as the most sensitive, and were used for calibration across the 1995–2003 period.
305 Table 1 shows the description of these, including, initial value, minimum, maximum and
306 calibrated value ranges of the hydrologic modeling for the Tapacurá River basin. The rank
307 order parameter sensitivity was defined based on the results presented in Figure 5. During the
308 validation process, the adjusted parameter values in the calibration phase were inserted in
309 SWAT, and new simulations were achieved with these calibrated parameters.

310

311 Table 1. Selected parameters after the sensitivity analysis of the SWAT model

Parameter	Description	Process	Initial value	Adjustment variation			Adjustment value***
				Method**	Minimum	Maximum	
Sol_AWC (mm/mm)	Soil available water capacity (mm H_2O/mm soil)	Soils (.sol)	V*	%	± 25%		+11,13%
Sol_Z (mm)	Depth from soil surface to bottom of layer (mm)	Soils (.sol)	V	%	± 25%		+3,53%
Sol_K (mm/h)	Saturated hydraulic conductivity (mm/h)	Soils (.sol)	V	%	± 25%		−22,68%
Gw_Revap (dimensionless)	Groundwater "revap" coefficient (dimensionless)	Ground water (.gw)	0.02	=	0.02	0.2	0.1643
Slsubbsn (m)	Average slope length (m)	Concentration time (.hru)	V	%	± 25%		+3,53%
Canmx (mm)	Maximum canopy storage (mm)	Evapotranspiration (.hru)	0	=	0	10	8.785
Gw_Delay (days)	Aquifer recharge time (days)	Ground water (.gw)	31	+	−30	60	42.945
Gwqmn (mm)	Threshold depth of water in the shallow aquifer required for return flow to occur (mm)	Ground water (.gw)	0	=	0	1.000	776.5
CN2 (dimensionless)	Curve Number for normal antecedent moisture conditions (dimensionless)	Surface runoff (.mgt)	V	%	± 10%		−8,31%
Alpha_BF (days)	The baseflow recession constant (days)	Ground water (.gw)	0.048	=	0	1	0.2025

312 *V: varies spatially. Its value is related to each use, type of soil and slope. **The methods are (a) percentage
313 variation (%), when the adjustment value varies in percentage in relation to the initial values of the parameters
314 that have spatial variability (V), (b) equality method (=), when the initial value of the parameter (only parameters
315 that are spatially unvaried) is replaced by the adjustment value obtained after the calibration phase, and (c)
316 addition method (+), when the value obtained after the calibration phase is added to the initial value of the
317 parameter. ***These are the variations obtained for each parameter after the calibration phase, which are applied
318 to the initial values of each parameter.

319

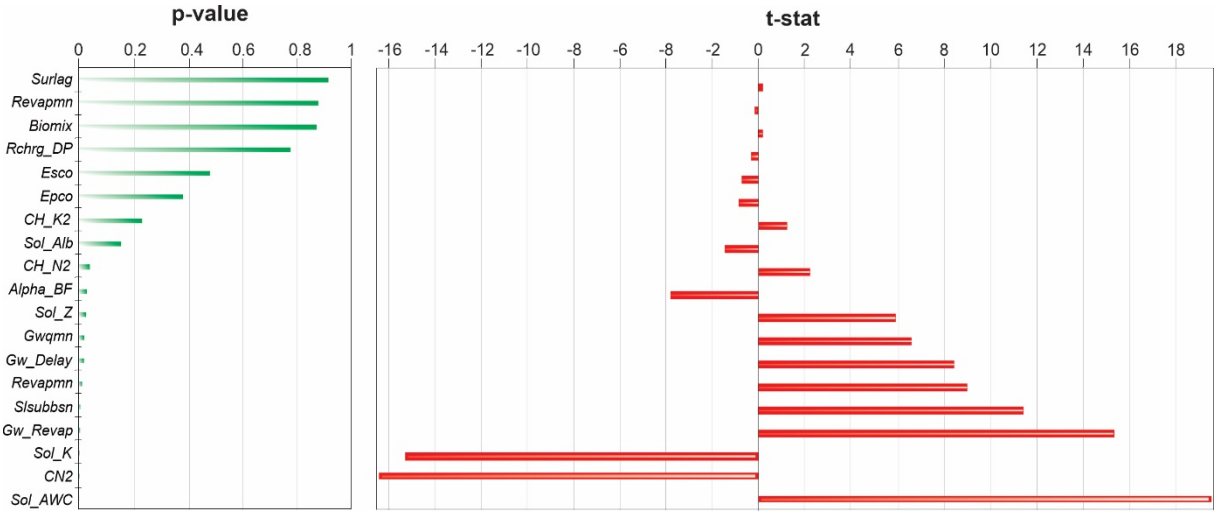

Figure 5. Result of the sensitivity analysis of the SWAT model parameters for the Tapacurá River basin

The *t*-stat (Figure 5) indicates the degree of sensitivity, and the higher its absolute value, the more sensitive the parameter is. The *p*-value, on the other hand, determines the significance of the sensitivity of the parameters, with values close to zero showing greater significance in the specific modeling (Abbaspour, 2012). Thus, the 10 parameters that had a *p*-value less than 0.1 were considered more sensitive.

From the 10 parameters considered most sensitive for the streamflow calibration (Table 1), four are related to groundwater (*Gw_Revap*, *Gw_Delay*, *Gwqmn*, *Alpha_BF*), three are related to the physical characteristics of the soil (*Sol_AWC*, *Sol_K* and *Sol_Z*), *Slsubbsn* related to the time of concentration, *Canmx* related to the evapotranspiration process and *CN2* related to the runoff. *Sol_AWC*, *CN2*, *Sol_K*, *Sol_Z* and *Slsubbsn* parameters influence the generation of surface runoff. *Gw_Revap*, *Gw_Delay*, *Gwqmn* and *Alpha_BF* parameters influence the baseflow, and *Canmx* influences the evapotranspiration. The parameters identified in this study as the most sensitive for the streamflow calibration have also been identified in previous studies in Brazilian river basins, as shown in Table 2. It is observed that the most sensitive parameters for the streamflow calibration in river basins do not vary much, differing little from one basin to another, regardless of the studied region. It was detected in this brief review of the literature, that the parameters identified as the most sensitive for the flow calibration by the SWAT model, for the Tapacurá River basin, correspond to at least five parameters of the studies by Strauch et al. (2012) and Andrade et al. (2013), and to seven in the studies by Melo Neto et al. (2014), Castro (2013) and Ferrigo (2014).

345 Table 2. More sensitive parameters for the calibration of the SWAT model, identified in other
346 studies in Brazil

Parameters	Quantity of correspondent parameters	Source	Region of Brazil
Alpha_BF , Canmx, CH_K2, CH_N2, Esco, Gw_Delay, Gw_Revap, Gwqmn, Revapmn, Sol_Z, Surlag	6	Aragão *et al*. (2013)	Northeast
Surlag, Alpha_BF, Sol_K, Gwqmn, CN2, Slsubbsn, CH_K2, Rchrg_DP, Esco, Sol_AWC, Sol_Z	7	Castro (2013)	West
CH_N2, CN2, Alpha_BF, Canmx, CH_K2, Epco, Esco, Gw_Delay, Gwqmn, Surlag	5	Strauch *et al*. (2012)	
CN2, Alpha_BF, Gw_Delay, Gwqmn, Gw_Revap, Esco, Sol_AWC, Sol_K, Sol_BD, Shallst, Gwht, Deepst, Revapmn, Anion_Excl	7	Ferrigo (2014)	
CN2, Sol_K, Sol_AWC, Canmx, Surlag, Gwqmn, Gw_Revap, Gw_Delay, Alpha_BF, Esco, CH_K2, CH_N2	6	Fukunaga (2012)	Southeast
Esco, Alpha_BF, Epco, Sol_Z, Canmx, CH_K2, Sol_AWC, Sol_K, CN2	6	Lelis *et al*. (2012)	
CN2, Alpha_BF, Rchrg_DP, Esco, Sol_Z, Sol_AWC, Sol_K	5	Andrade *et al*. (2013)	
Alpha_BF, CN2, Gwqmn, Esco, Sol_Z, Sol_AWC, CH_N2, Blai, Canmx, Gw_Revap	7	Melo Neto *et al*. (2014)	
Esco, Alpha_BF, CH_K2, Canmx, Sol_Awc, Sol_K, CN2, Slope, Blai, Gwqmn	6	Bonumá *et al*. (2010)	South
CH_K2, Slope, Esco, Alpha_BF, Sol_Z, Sol_K, Sol_AWC, Surlag, CN2, CH_N2	6	Baltokoski *et al*. (2010)	
Esco, Alpha_BF, Sol_Z, Sol_AWC, Blai, Gwqmn, Revapmn, CH_K2, CN2, GW_Revap	6	Malutta (2012)	

347

348 **3.2 Set-up and validation of the SWAT model**

349 **3.2.1 Baseline streamflow (1995-2013)**

350 Table 3 shows the statistical analysis and performance of the model after the calibration and
351 validation for observed and simulated streamflow. Based on the R^2 and NSE criteria of
352 Moriasi et al. (2007), the calibration of streamflow showed good performance, and
353 satisfactory performance in relation to the PBIAS. The validation, on the other hand,
354 surpassed the indices obtained during the calibration, showing a better adjustment of the
355 observed and simulated hydrographs, and a better representation of peak flows, base flow and
356 median flows (Figures 6a-6b). The R^2 and NSE values obtained during validation can be
357 classified as very good, and the PBIAS value as good (Figures 6c-6d). These results are

similar to those obtained by Montenegro and Ragab (2012) and Ribeiro Neto et al. (2014), who performed hydrological simulations with the DiCaSM and MODHAC models, respectively, for the Tapacurá River basin.

Table 3. Results of hydrologic modeling using SWAT model for Tapacurá River basin

Statistics	Streamflow (m³/s)			
	Calibration		Validation	
	Simulated	Observed	Simulated	Observed
Mean	1.59	1.29	2.09	2.34
Maxima	12.29	16.34	33.93	29.17
Minima	0.00	0.00	0.00	0.00
Standard deviation	2.45	2.68	5.11	4.45
R^2	0.72		0.86	
NSE	0.71		0.85	
PBIAS	−23.73		−11.94	

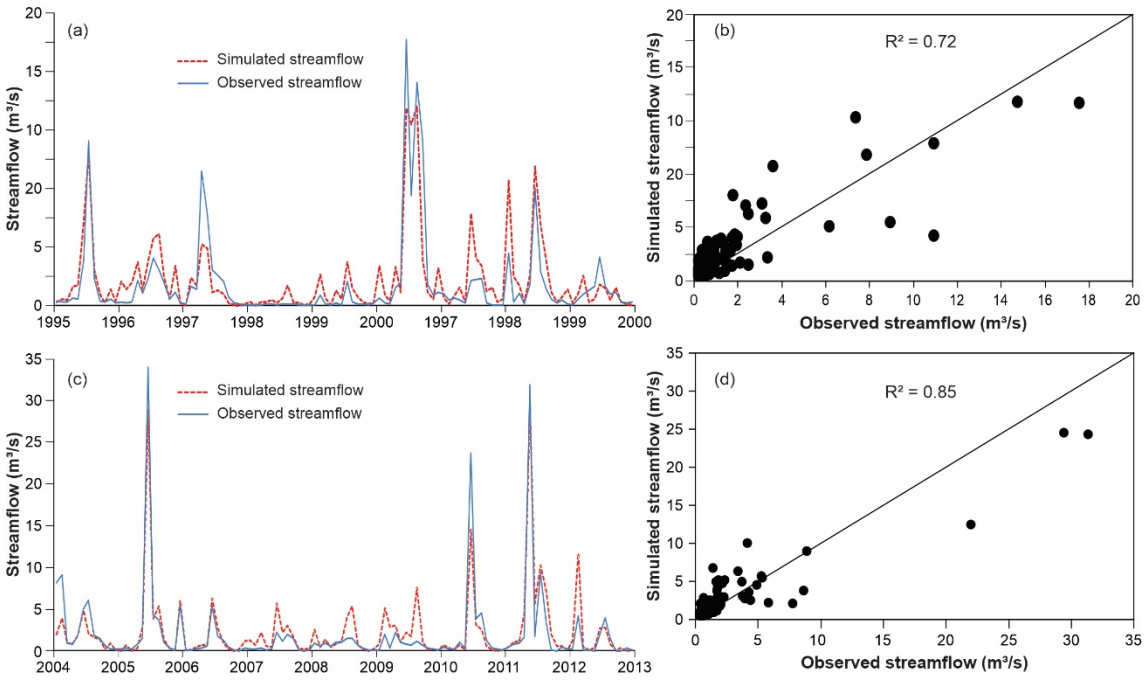

Figure 6. (a) Observed and simulated monthly streamflows for calibration period, (b) observed and simulated scatter plot for calibration period, (c) observed and simulated monthly streamflows for validation period, and (d) observed and simulated scatter plot for validation period from the Tapacurá River basin.

Figure 7 presents the uncertainty analysis results of SUFI-2 during the calibration and validation periods at the Vitória de Santo Antão streamflow gauge. In this figure, the shaded

region (95% probability uncertainty plot - 95PPU) contains all uncertainties from the different sources. The results for the streamflow gauge show that most (84%) of the observed data were bracketed by the 95PPU. The results show that although some peak values were missing from the 95PPU band, the SWAT model was however capable of simulating large flows and extreme events in the river basin. This shows that the SUFI-2 algorithm captured the observed data well for the streamflow gauge but had high uncertainty for simulated peak values. In addition, the results obtained show that calibration of the SWAT model in this basin is challenging due to the uncertainties that are driven by the streamflow process, which are not totally understood.

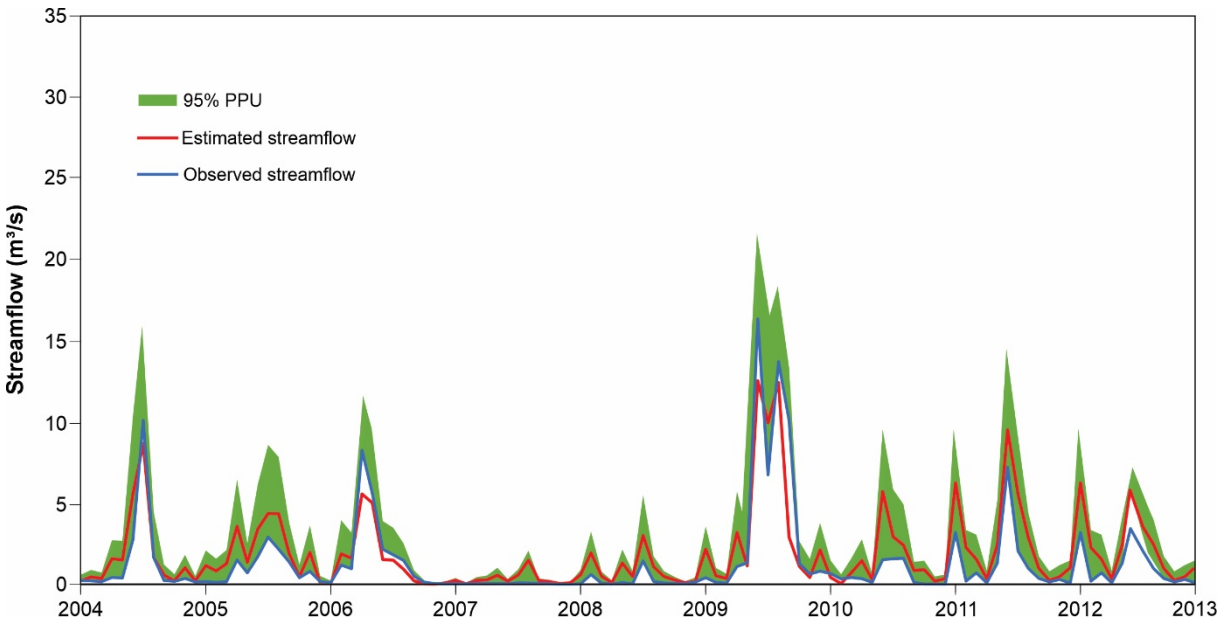

Figure 7. 95% probability uncertainty plot of observed and simulated streamflow

The results indicated that the p-factor and r-factor values during the calibration were 0.22 and 0.33, respectively. These results can be considered good in terms of the percentage of data being bracketed (p-factor), but the uncertainties are larger as expressed by the r-factor for calibration, showing higher uncertainty in discharge peaks. The parameter uncertainties were tolerable when the parameter ranges of the NS and R^2 reached the desired limits. When

390 the NSE value is >0.60, the results are satisfactory, and once NSE is >0.75, the simulation
391 results are good (Nash & Sutcliffe, 1977). For the results during the calibration, the values of
392 R^2 and NS were 0.78 and 0.75, respectively. The results indicate that the model can be
393 accepted for the Tapacurá River basin.
394
395 **3.2.2 Baseline sediment yield (1995-2013)**
396 The modeled mean sediment yield results were very close to the observed mean value,
397 showing a mean difference of only −0.69 t, with R^2 = 0.77, NSE = 0.69 and PBIAS = 21.68
398 (Table 4), which can be considered as good. The results are close to those obtained by da
399 Silva et al. (2012) and dos Santos et al. (2015), who estimated sediment yield for this basin
400 based on the universal soil loss equation and its modified version, respectively, for the
401 Tapacurá River basin.
402
403 **Table 4.** Results of modeling sediment yield

Statistics	Simulated sediment yield (t/ha/year)	Observed sediment yield (t/ha/year)
Mean	2.49	3.18
Maxima	6.18	7.42
Minima	0.37	0.11
Standard deviation	2.29	3.03
R^2	0.77	
NSE	0.69	
PBIAS	21.68	

404
405 **3.3 Streamflow and sediment yield for Tapacurá River basin**
406 After calibration and validation for the current conditions of climate and LULC, streamflow
407 and sediment yield for the Tapacurá basin were compared (Table 5). The results show that
408 sediment yield in the basin is directly related to rainfall, indicating that this region has a fast
409 flow response. The highest values occurred in 2005 and 2011. The lowest estimated sediment
410 yield occurred in 1998, which registered the lowest rainfall and corresponding flow for the

411 entire analyzed period. The results show a marked variation in the standard deviation for
412 streamflow and sediment yield data, equal to 83.25 mm and 11.48%, respectively. The
413 coefficient of variation similarly shows marked variation of above 60% during the period
414 analyzed. Figure 8a represents the spatial distribution of sediment yield in the sub-basins. The
415 results show that sediment yield was higher in the eastern sub-basins due to the predominance
416 of areas with sugarcane cultivation in undulating terrain, and the influence of higher rainfall
417 (Figure 8b), resulting in higher streamflow (Figure 8c), contributing in turn, to accelerated
418 erosion in these sub-basins.

419

420 **Table 5.** Annual averages of rainfall, streamflow and sediment yield

Year	Rainfall (mm)	Streamflow (mm)	Sediment yield (t/ha/year)
1995	817.26	74.62	7.80
1996	993.81	105.61	18.44
1997	770.63	102.90	14.21
1998	427.16	5.84	0.25
1999	582.25	29.79	4.40
2000	1396.87	237.65	30.20
2001	831.03	58.33	5.83
2002	995.98	114.96	18.46
2003	639.97	42.03	7.88
2004	886.84	131.73	23.65
2005	1159.85	239.62	35.16
2006	728.63	65.46	9.44
2007	841.53	78.10	11.42
2008	786.33	75.58	16.83
2009	878.35	100.04	25.33
2010	897.69	154.98	16.88
2011	1482.81	338.31	41.21
2012	730.46	96.45	31.67
Mean	**880.41**	**114.00**	**17.73**
Standard deviation	**261.31**	**83.25**	**11.48**
Coefficient of variation (%)	**29.68**	**73.03**	**64.78**

421

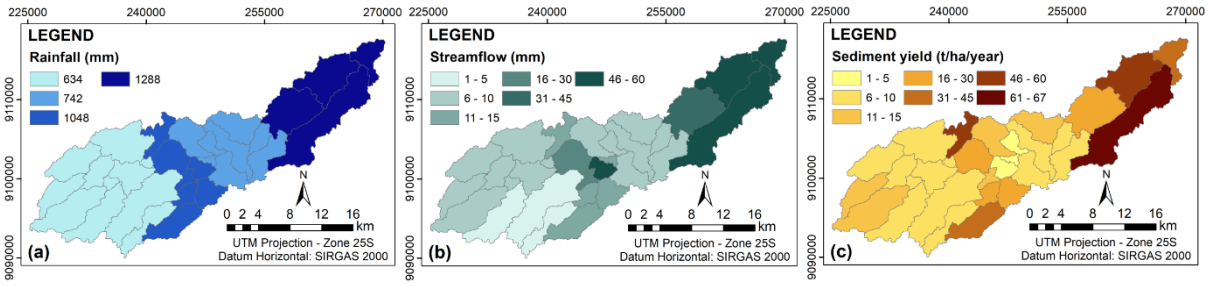

Figure 8. Maps of spatial distribution: (a) streamflow, (b) rainfall, and (c) sediment yield for Tapacurá River basin.

3.4 Estimating future LULC in the Tapacurá River basin by 2050

Figures 9a and 9b show the prediction of the LULC for 2050 estimated by the MP algorithm and spatial validation of simulated LULC for Tapacurá River basin in 2015, respectively. The kappa statistics for LULC classifications in 1989, 2007 and 2015 showed good agreement between the classified map of each year and the mesh equaled 0.81, 0.79, and 0.82, respectively. The matrix of the transition probability of LULC for 2007 and 2015 is shown in Table 6. The diagonal matrix results show the percentages of persistence, while the other values correspond to the percentages of change from one LULC class to another. The water, urban area, and sugarcane classes had a probability of persistence greater than 80%. However, the highest probability of change was from the livestock to the sugarcane class.

Table 6. Matrix of the transition probability of LULC classes for 2007 and 2015 in the study area.

2007	2015						
	Caatinga	**Livestock**	**Rain forest**	**Water**	**Agriculture**	**Urban area**	**Sugarcane**
Caatinga	0.2394	0.1682	0	0.0054	0.5075	0.0152	0.0643
Livestock	0.0356	0.2693	0	0	0.5719	0.0411	0.0821
Rain forest	0.0029	0.2356	0.6108	0.1005	0	0	0.0501
Water	0.0123	0.0066	0.0343	0.8489	0.0757	0.0173	0.0049
Agriculture	0.2479	0.1237	0.0546	0	0.5242	0	0.0496
Urban area	0	0.0018	0	0.0001	0.0051	0.9930	0
Sugarcane	0	0.1244	0.0015	0.0002	0	0	0.8739

The areas with the most forecast hits comprised the greater part of the central portion of study area, where agriculture and sugarcane classes predominate (predicting hits). Most prediction failures (misses) were found in the border of the study area. For the western region of the catchment, the forecasting resulted in class changes, but these did not suggest considerable changes (false alarms).

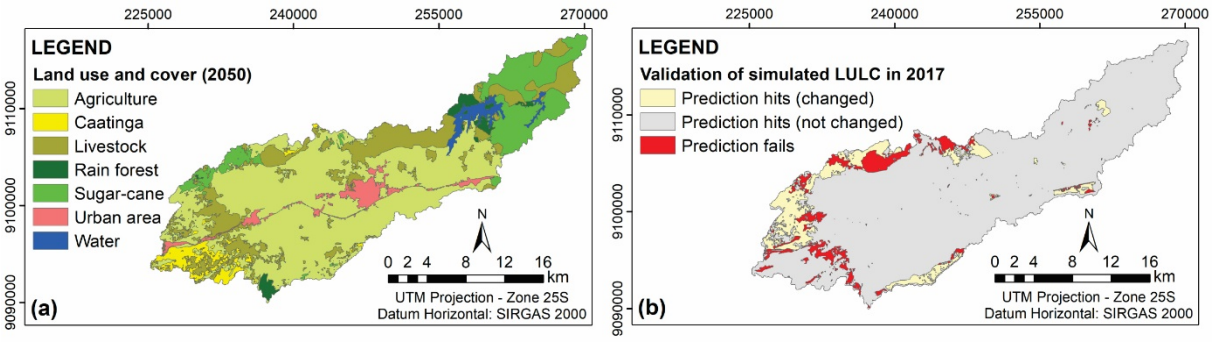

Figure 9. (a) LULC map for the Tapacurá River basin for 2050, and (b) spatial validation of simulated LULC in 2015.

Table 7 shows the areas for each LULC identified in the Tapacurá River basin and the percentage of change in the area for the two studied scenarios for 2050. The modeling results show an increase in agriculture and sugarcane classes, and a decrease in the livestock (−87.01%) and rain forest (−17.27) classes. These results are corroborated by Xavier and Silva (2018), who pointed out that forest cover has been reducing since the 1970s due to the expansion of agriculture and sugarcane, mainly in the southwestern and eastern portion of the basin, with the latter being the most occupied by sugarcane. Table 8 presents the modeled LULC for the study area in 2015 and confusion matrix with omission and commission errors found by comparing the classification. The class that showed the largest omission error and commission were Caatinga and livestock. The values show counts of pixels that have been wrongly included in a category. The agriculture and sugarcane classes showed the best results

461 when compared to the others, because they are the classes that had the greatest area of growth
462 and therefore the least error in the estimated areas.
463
464 **Table 7.** Change in two LULC scenarios in the Tapacurá River basin for 2050.

LULC	Optimistic		Pessimistic		Change
	Area (km²)	Area (%)	Area (km²)	Area (%)	(%)
Agriculture	180.89	38.47	252.19	53.66	71.30
Livestock	182.30	38.77	95.29	20.27	−87.01
Sugarcane	53.60	11.40	65.55	13.95	11.95
Rain forest	27.38	5.82	10.11	2.15	−17.27
Urban areas	10.36	2.20	18.34	3.90	7.98
Water	10.50	2.23	10.60	2.26	0.10
Caatinga	5.13	1.09	17.92	3.81	12.79
Total	**470**	**100**	**470**	**100**	**–**

465
466 **Table 8.** Matrix of omission and commission errors.

LULC	Caatinga	Livestock	Sugarcane	Rain forest	Water	Agriculture	Urban area	Omission (%)	Commission (%)
Caatinga	16861	4435	239	39	85	6040	456	40.11	21.91
Livestock	1947	78039	1251	228	235	8803	342	14.10	20.78
Sugarcane	0	726	54905	172	348	35	4	2.29	9,16
Rain forest	2	270	234	9269	246	209	0	9.39	9.83
Water	0	254	454	307	9973	124	0	10.25	10.13
Agriculture	2771	14464	3806	189	210	248983	2954	8.92	6.59
Urban area	12	322	0	0	0	2359	13975	16.16	21.18

467
468 **3.5 Evaluation of downscaling for future climate scenarios**
469 In this section, the comparison of HadGEM2-ES model with observed rainfall data is shown.
470 Figure 10 shows the comparison between observed and downscaled average monthly rainfall
471 (RCPs 4.5 and 8.5). The average R^2 values was 0.93, thereby indicating better correspondence
472 between downscaled and observed data after bias correction.
473

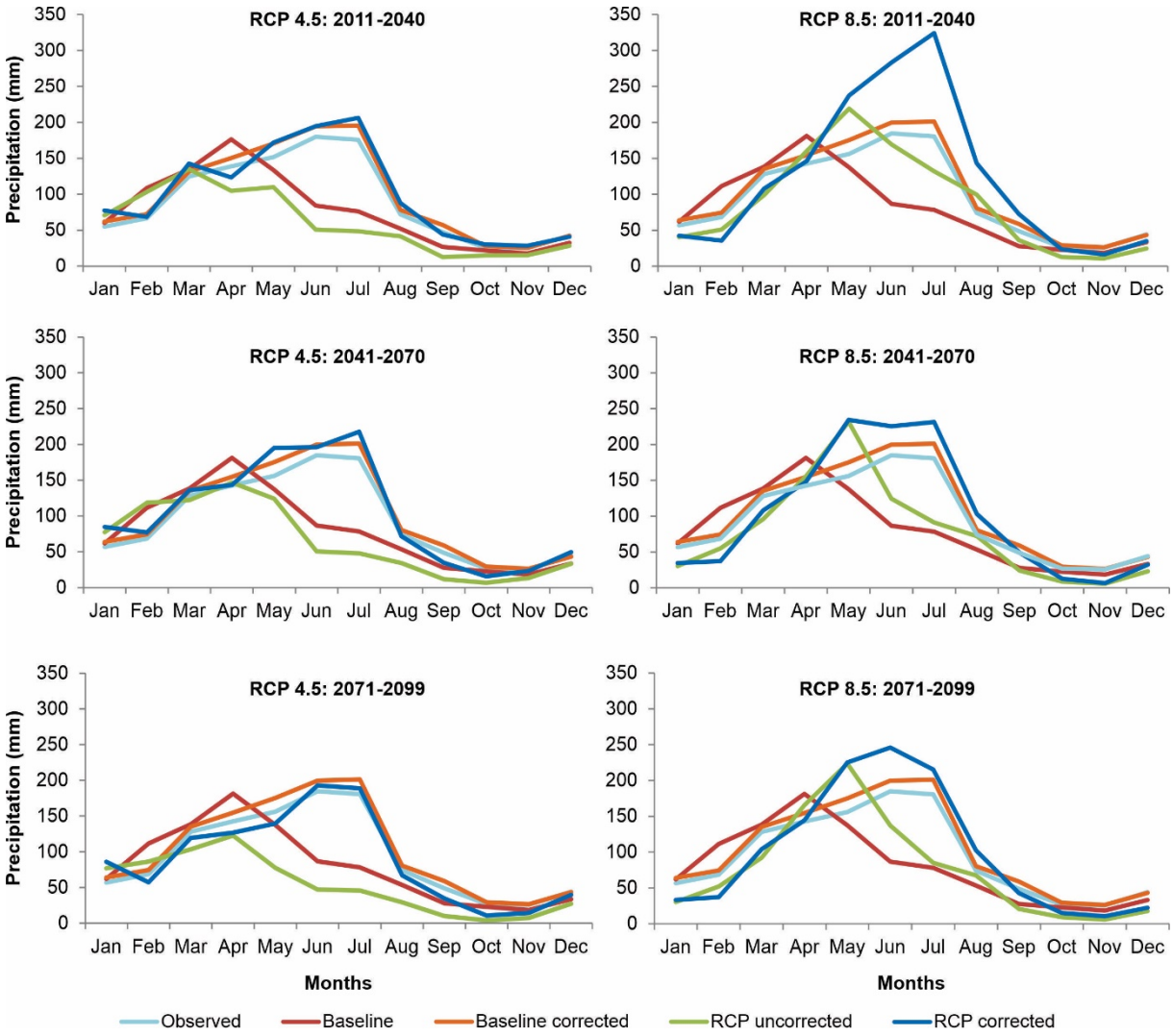

Figure 10. Bias correction of future, baseline, and observed rainfall data for RCPs 4.5 and 8.5.

3.6 Combined impacts of climate change and LULC on streamflow and sediment yield

Runoff-erosion processes for the Tapacurá River basin were estimated using two different land use scenarios (optimistic and pessimistic), driven by two RCPs (4.5 and 8.5). The rainfall in all other periods was higher than the rainfall of the baseline period (1995–2012), for both RCPs (Table 9). Streamflow based on RCP 4.5, and LULC optimistic, had an increase relative to the base period (1995-2012) of 79, 104 and 63%, respectively in the periods 2011–2020, 2041–2070 and 2071–2099. Based on RCP 8.5, the expected streamflow exceeded that

485 observed in the base period by 217% in the period 2011–2040, 145% in 2041–2070 and 119%
486 in the three past decades (2071–2099), due to the increase in the estimated rainfall in relation
487 to RCP 4.5.

488 In this study, the SWAT hydrological model driven by climate simulations estimated an
489 overall increase in the Tapacurá River flow for optimistic and pessimistic scenarios. The
490 results obtained showed that the average annual simulated streamflow will increase mainly
491 between 2014–2040 in the RCP 8.5, while in the RCP 4.5 presented the lower values.
492 Between 2041–2070 and 2071–2099 there is less variation between RCPs and scenarios, but
493 also with an increase in values in relation to the baseline. The results of annual simulated
494 streamflow showed an increase in the optimistic scenario in the two climatic scenarios (RCP
495 4.5 and RCP 8.5). The greatest values were obtained using the RCP 4.5 scenario, whose
496 values were greater by 8.2% in 2014–2040, 12.2% in 2041–2070, and 15.0% in 2071–2099.
497 This result is clearly sensitive to the result of future climate projections. Silva et al. (2012)
498 and Santos et al. (2015) stated that the increase in river streamflow in the future depends
499 mainly on increases in precipitation and decreases in temperature and evapotranspiration in
500 this basin.

501

502 **Table 9.** Annual averages of rainfall, streamflow and sediment yield in different scenarios of
503 climate change and LULC

LULC	Processes	Baseline*	RCP 4.5			RCP 8.5		
		1995–2012	2014–2040	2041–2070	2071–2099	2014–2040	2041–2070	2071–2099
	Rainfall (mm)	880.41	1194.43	1244.41	1078.88	1487.20	1222.70	1200.81
Optimistic	Streamflow (mm)	114.00	204.57	232.82	185.87	361.64	278.96	249.72
	Sediment yield (t/ha/year)	17.73	36.95	38.517	32.00	51.42	38.519	36.69
Pessimistic	Streamflow (mm)	–	208.13	246.88	195.10	369.57	295.78	265.93
	Sediment yield (t/ha/year)	–	59.13	67.67	52.55	93.65	74.02	69.22

504 *Baseline: period used for hydrologic modeling in the SWAT model.

505

506 As expected, sediment yield in the basin showed the same trend as streamflow in both
507 climate change scenarios. The projected sediment yield values for RCP 4.5 exceeded those of

508 the baseline by between 80 and 117%. For RCP 8.5, the values were even higher, varying
509 between 107 to 190% for the different periods of analysis. The pessimistic LULC scenario
510 showed increases in sediment yield for all years and RCPs relative to the optimistic. These
511 results serve as an urgent call for the adoption of mitigating measures to avoid associated
512 environmental problems and improve the management of land and water resources.

513 The streamflow in the pessimistic scenario, for RCP 4.5 exceeds the optimistic scenario
514 by 2% in the period 2011–2040, 6% in the period 2041–2070 and 5% in the period 2071–
515 2099. Sediment yield varies by 60, 76 and 64% across the periods. The streamflow results for
516 the pessimistic scenario RCP 8.5 show a slight increase of between 2 to 6% when compared
517 to the optimistic scenario. The sediment yield increase ranged between 60 and 76%, showing
518 that soil erosion in the region is more sensitive to climate variability than streamflow, and that
519 LULC changes can have serious impacts on the basin.

520 The highest values of streamflow and sediment yield in the RCP 4.5 scenarios occurred
521 in 2041–2070, while in the RCP 8.5 scenarios, the highest values occurred in the first part of
522 the century (2014–2040). This trend is related to the rainfall pattern of the RCP 4.5 and 8.5
523 scenarios, as in RCP 4.5 the rainiest period is 2041–2070, and in RCP 8.5 it is 2014–2040.
524 The results suggest that even in the near (2014–2040) to medium (2041–2070) future there
525 may be negative impacts on the dynamics of the Tapacurá River basin, as well as for the
526 RMR, including floods, silting in rivers and reservoirs, and reducing the productive capacity
527 of the soils.

528 Figure 11 shows the results of streamflow and sediment yield estimated for Tapacurá
529 reservoir using future climate data. Based on SWAT model projections, the results show an
530 increase in sediment yield for the analyzed LULC scenarios and climate change. These values
531 suggest decision makers responsible for storage management in the Tapacurá Reservoir must
532 implement measures for the effective management of the stored volume, as the reservoir plays

a significant role in the regional hydrology and for water management for the Caatinga/Atlantic forest ecotone region, including amelioration of flood events in the RMR.

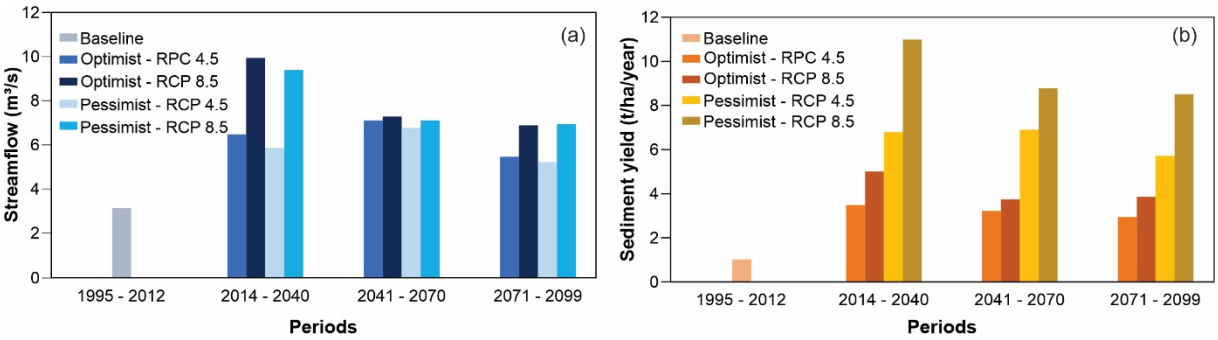

Figure 11. Streamflow (a) and sediment yield (b) estimated for Tapacurá reservoir.

4. Discussion

This study has analyzed the impact of climate and LULC change on streamflow and sediment yield in the Tapacurá River basin, using a combination of two models (climate and hydrological), which allowed a more integrated assessment of water balance and sediment dynamics. Previous studies have focused on different components of the Tapacurá river Basin. For instance, Silva e al. (2010a) studied the spatiotemporal variability and precipitation pattern for this basin and reported a warming trend in northeastern Brazil and a decreasing trend in rainfall in Tapacurá River basin between 1970–2000 and an increase from 2000–2010. Silva et al. (2010b) and Silva et al. (2012) analyzed vegetation cover, sediment yield, soil loss, and prioritization of critical sub-catchments in the Tapacurá River basin based on remote sensing and Geographic Information System. Silva et al. (2014) predicted soil erosion and sediment yield in the Tapacurá catchment using an empirical model, whereas Xavier and Silva (2018) implemented a GIS-based method for temporal dynamic modelling of the land use and land cover. Montenegro and Ragab (2012) analyzed the impact of possible climate and land use changes in the Brazilian semi-arid region, while Dos Santos et al. (2015)

554 investigated historic land cover and climate change effects on streamflow and sediment yield
555 for the Tapacurá River basin specifically. Although these studies have provided useful
556 contextual understanding and methodological advances, what has been lacking is an
557 integrated evaluation of the effects of LULC change on streamflow and sediment yield, within
558 the context of alternative climate change scenarios. Furthermore, previous studies have
559 analyzed certain aspects of the climate and land, using different input data quality, methods
560 and assumptions, hindering the comparison of results between studies. Like Tapacurá River
561 basin is a strategic basin in the Caatinga/Atlantic forest ecotone of Northeastern Brazil, an
562 assessment of future climatic and hydrological conditions is essential for water management
563 for this basin. Several applications of LULC change and climate change models with SWAT
564 model has been used for predicting the hydrologic response (Strauch et al., 2012; Čerkasova
565 et al., 2018; Tamm et al., 2018; Silva et al., 2018; Chen et al., 2019; Bhatta et al., 2019).
566 Using a combination of SWAT model and climate model a more realistic description of the
567 processes taking place in the Tapacurá River basin. The hydrological model gave some
568 answers on the relative importance of LULC versus climate change effect on streamflow. The
569 combined impact of climate variability and LULC changes on water resources under present
570 and future scenarios were evaluated with multiple projections using both RCP 4.5 and 8.5
571 scenarios. However, a limitation of this study is the use of a single hydrological model and a
572 single regional climate model. The application of multi-model techniques might improve
573 understanding of uncertainty arising from model selection. Another limitation of this study is
574 that static LULC maps were used to represent baseline and future periods. In the future,
575 additional LULC maps must be considered to circumvent scenario-based ambiguity.

576 The results over the studied period using the projected datasets indicate that this basin
577 clearly presents a high variability during the studied period, and further that precipitation does
578 not show a uniform trend in past observation or in future projections, and that the pessimistic

579 and optimistic climate scenarios also yielded higher flows than those of the baseline.
580 Moreover, studies using regional circulation models showed a systematic decrease of total
581 precipitation in northeastern Brazil, as reported by Oyama and Nobre (2004), Souza and
582 Oyama (2011), Feron et al. (2019), and Marengo et al. (2020), runoff (Lapola et al., 2019;
583 Avila-Díaz et al., 2020) and sediment yield (Rodriguez-Lloveras et al., 2016), when compared
584 with the present behavior of the basin over the baseline period.

585 Additionally, as can be seen in the projected data, the bias correction is having the effect
586 of increasing winter rainfall relative to baseline for the first two periods, which is probably
587 why there are bigger increases in modelled flow and sediment for these periods, relative to the
588 final period. The results of streamflow and sediment yield are influenced by the model used,
589 and the bias correction selected in the modeling. Furthermore, this study is limited to
590 simulations on a monthly scale, due to the low performance of the model for simulations on a
591 daily scale for this basin. Poor simulations at daily scale arise due to the high climatic
592 variability, soil types and LULC in this basin, as presented in Silva et al. (2014), and Xavier
593 and Silva (2018). However, these results are in agreement with other hydrological projections
594 in the Brazilian semiarid region (Santos et al., 2016). Relative to historical conditions,
595 therefore, higher flows and sediment yields in this basin can be anticipated. These results
596 serve to alert decision makers of the value in using hydrological models such as SWAT to
597 highlight potential changes in the behavior of flows and sediment yield.

598 Another point to be highlighted is the uncertainties regarding the behavior of the climate
599 in this portion of Brazil, which is marked by the low quality of the prediction of climatic data
600 (Silva et al., 2010a), especially for the long-term due to recurrent periods of drought in the
601 region (Silva et al., 2010b; Santos et al., 2020). As for the simulations of LULC, it should be
602 noted that this basin has had a high rate of change in LULC in recent decades, due to the
603 increase in monocultures such as sugar cane, and more recently with the increased livestock

(De Carvalho et al., 2015; Santana et al., 2019), which increase the uncertainties in the LULC scenario estimates. However, there is a lack of studies on modeling the impacts of future LULC and climate change on runoff and sediment yield for the Tapacurá River basin, as well as for the entire portion of the coastal area of northeastern Brazil, which can be used by decision makers on availability/consumption of water for economic activities and for the population of the basin. Future studies using other GCMs are necessary to improve the simulation of precipitation in northeastern Brazil, including for example, the effect of different domain sizes and grid spacing. Despite these uncertainties, the SWAT model results have contributed to developing a better understanding of runoff and sediment behavior in the Tapacurá River basin.

5. Conclusions

This paper investigated the impacts of climate change on streamflow and sediment yield in the Tapacurá River basin. The SUFI-2 algorithm was used for the calibration and validation of the SWAT model, driven by bias corrected, downscaled climate projections under projected land use change scenarios. The hydrologic modeling represented the runoff-erosion processes for the Tapacurá River basin effectively, with results achieving a 'good' threshold (Moriasi et al. 2007). Streamflow and sediment yield processes were more intense in sub-basins that have predominant coverage of sugarcane in undulating terrain.

The projected LULC changes for 2050 were mainly reductions in the livestock and rain forest classes and their replacement by agriculture and sugarcane classes. This was observed almost across the entire basin. The LULC projections based on the MP algorithm showed acceptable values, with a good kappa statistic and an AUC of 0.71, which is considered good quality for simulations.

Mean streamflow and particularly sediment yield of the basin are expected to rise considerably under RCP 8.5, partly in response to likely increases in mean rainfall. Simulations indicated highest erosion for the pessimistic scenario under RCP 8.5, followed by the pessimistic scenario and RCP4.5. Lower sediment yields occurred for the optimistic and RCP 8.5, with lower still for the optimistic and RCP 4.5. However, the latter is still considerably higher than baseline. The results show that despite the uncertainties present in the simulations of climate change impacts, the basin may experience serious environmental, and water availability problems linked to severe climatic conditions.

Based on our findings, the Tapacurá Reservoir will experience an increase in streamflow for both scenarios of LULC and climate change. Although this may lead to an increase in the reservoir water availability, the associated increase in sediment yield means there is also a considerable increase in the risk of silting, with a consequent decrease in storage capacity and reduced flood protection during extreme events. In recent decades, considerable changes in LULC due to an increase of livestock and agriculture have already altered the streamflow and sediment yield of the Tapacurá River basin at both seasonal and long-term time scales. As the pressure for LULC changes in the Tapacurá River basin continue to grow, evaluation of its impacts on the projected runoff-erosion regime of the basin must be systematically integrated into decision-making for water, land and biodiversity management in the basins in the Caatinga/Atlantic forest ecotone of Brazil.

Acknowledgements

This study has been jointly supported by FACEPE and FINEP (REHIDRO 1830). The authors are supported by CNPq, and ANA (National Water and Sanitation Agency) is acknowledged for providing data sets. This study was also financed in part by the Brazilian Federal Agency for the Support and Evaluation of Graduate Education (Coordenação de Aperfeiçoamento de

653 Pessoal de Nível Superior - CAPES) – Fund Code 001, and National Council for Scientific
654 and Technological Development, Brazil – CNPq (Grant Nos. 304213/2017-9 and
655 304540/2017-0).

656

657 **References**

658 Abbaspour KC, Yang J, Maximov I, Siber R, Bogner K, Mieleitner J, Zobrist J, Srinivasan R (2007)
659 Modelling hydrology and water quality in the pre-alpine/alpine Thur watershed using SWAT. Journal
660 of Hydrology, 333: 413– 430. https://doi.org/10.1016/j.jhydrol.2006.09.014

661 Ahmadlou M, Delavar MR, Tayyebi A (2016) Comparing ANN and CART to model multiple land use
662 changes: a case study of Sari and Ghaem-Shahr cities in Iran. Journal of Geomatics Science and
663 Technology, 6(1), 292-303.

664 Alvalá RCS, Dias MCA, Saito SM, Stenner C, Franco C, Amadeu P, Ribeiro J, Santana RASM, Nobre
665 CA (2019) Mapping characteristics of at-risk population to disasters in the context of Brazilian early
666 warning system. International Journal of Disaster Risk Reduction, 41, 101326.
667 https://doi.org/10.1016/j.ijdrr.2019.101326

668 An C, Zhu R, Wang X, Long Y, Lu Y, Chen Y, Zhong H (2020) The correlation analysis of RCPs
669 impeller geometrical parameters and optimization in coast-down process. Annals of Nuclear Energy,
670 142, 107283. https://doi.org/10.1016/j.anucene.2019.107283

671 Andrade MA, Mello CR, Beskow S (2013) Simulação hidrológica em uma bacia hidrográfica
672 representativa dos Latossolos na região Alto Rio Grande, MG. Revista Brasileira de Engenharia
673 Agrícola e Ambiental, 17(1): 69-76.

674 Aragão R, Cruz MAS, Amorim JRA, Mendonça LC, Figueiredo EE, Srinivasan VS (2013) Análise de
675 sensibilidade dos parâmetros do modelo SWAT e simulação dos processos hidrossedimentológicos em
676 uma bacia no agreste nordestino. Revista Brasileira de Ciência do Solo, 37: 1091-1102.

677 Arnold JG, Srinivasan R, Muttiah RS, Williams JR (1998) Large area hydrologic modeling and
678 assessment – part I: model development. Journal of the American Water Resources Association, 34,
679 73–89.http://dx.doi.org/10.1111/j.1752-1688.1998.tb05961.x

680 Avila-Diaz A, Benezoli V, Justino F, Torres R, Wilson A (2020) Assessing current and future trends
681 of climate extremes across Brazil based on reanalyses and earth system model projections. Climate
682 Dynamics, 55, 1403–1426. https://doi.org/10.1007/s00382-020-05333-z

683 Baltokoski V, Tavares MHF, Machado RE, Oliveira MP (2010) Calibração de modelo para a
684 simulação de vazão e de fósforo total nas sub-bacias dos rios Conrado e Pinheiro – Pato Branco (PR).
685 Revista Brasileira de Ciência do Solo, 34: 253-261.

686 Bárdossy A, Pegram G (2011) Downscaling precipitation using regional climate models and
687 circulation patterns toward hydrology. Water Resources Research, 47(4), W04505.
688 https://doi.org/10.1029/2010WR009689

689 Behera S, Panda RK (2006) Evaluation of management alternatives for an agricultural watershed in a
690 sub-humid subtropical region using a physical process based model. Agriculture, Ecosystems &
691 Environment, 113, 62–72. https://doi.org/10.1016/j.agee.2005.08.032

692 Berg P, Feldmann H, Panitz HJ (2012) Bias correction of high resolution regional climate model data.
693 Journal of Hydrology, 448–449, 80-92. https://doi.org/10.1016/j.jhydrol.2012.04.026

694 Bhatta B, Shrestha S, Shrestha PK, Talchabhadel R (2019) Evaluation and application of a SWAT
695 model to assess the climate change impact on the hydrology of the Himalayan River Basin. Catena,
696 181, 104082. https://doi.org/10.1016/j.catena.2019.104082

697 Bonumá NB, Reichert JM, Minella JP, Barros CAP, Rodrigues MF, Buarque DC (2010) Balanço
698 hídrico e sua relação com a modelagem da produção de sedimentos em uma pequena bacia
699 hidrográfica rural. Proceedings of IX Encontro Nacional de Engenharia de Sedimentos. Brasília:
700 ABRH.

701 Braga ACFM, Silva RM, Santos CAG, Galvão CO, Nobre P (2013) Downscaling of a global climate
702 model for estimation of runoff, sediment yield and dam storage: a case study of Pirapama Basin,
703 Brazil. Journal of Hydrology, 498, 46-58. http://dx.doi.org/10.1016/j.jhydrol.2013.06.007

704 Brito CS, Silva RM, Santos CAG, Brasil Neto RM, Coelho VHR (2021) Monitoring meteorological
705 drought in a semiarid region using two long-term satellite-estimated rainfall datasets: A case study of
706 the Piranhas River basin, northeastern Brazil. Atmospheric Research, 250, 105380.
707 http://dx.doi.org/10.1016/j.atmosres.2020.105380

708 Carvalho NO (2008) Hidrossedimentologia prática. Rio de Janeiro: Editora Interciência. 599p.

709 Castro KB (2013) Avaliação do modelo SWAT na simulação da vazão em bacia agrícola do cerrado
710 intensamente monitorada. PhD. Dissertation, Universidade de Brasília, Brasília – DF, 117p.

711 Čerkasova N, Umgiesser G, Ertürkc A (2018) Development of a hydrology and water quality model
712 for a large transboundary river watershed to investigate the impacts of climate change – A SWAT
713 application. Ecological Engineering, 124, 99-115. https://doi.org/10.1016/j.ecoleng.2018.09.025

714 Chen Y, Li X, Liu X, Zhang W, Huang M (2019) Tele-connecting China's future urban growth to
715 impacts on ecosystem services under the shared socioeconomic pathways. Science of The Total
716 Environment, 652, 765-779. https://doi.org/10.1016/j.scitotenv.2018.10.283

717 Chen Y, Marek GW, Marek TH, Moorhead JE, Heflin KR, Brauer DK, Gowda PH, Srinivasan R
718 (2019) Simulating the impacts of climate change on hydrology and crop production in the Northern
719 High Plains of Texas using an improved SWAT model. Agricultural Water Management, 221, 13-24.
720 https://doi.org/10.1016/j.agwat.2019.04.021

721 Chou SC, Lyra A, Mourão C, Dereczynski C, Pilotto I, Gomes J, Bustamante J, Tavares P, Silva A,
722 Rodrigues D, Campos D, Chagas D, Sueiro G, Siqueira G, Marengo J (2014a) Assessment of climate
723 change over South America under RCP 4.5 and 8.5 downscaling scenarios. American Journal of
724 Climate Change, 3: 512-525.

725 Chou SC, Lyra A, Mourão C, Dereczynski C, Pilotto I, Gomes J, Bustamante J, Tavares P, Silva A,
726 Rodrigues D, Campos D, Chagas D, Sueiro G, Siqueira G, Marengo J (2014b) Evaluation of the Eta
727 simulations nested in three global climate models. American Journal of Climate Change, 3: 438-454.

728 Clark Labs (2020) About Clark Labs. Clark Labs. https://clarklabs.org. Accessed 10 August 2020

729 Collins, W.J., Bellouin, N., Doutriaux-Boucher, M., Gedney, N., Halloran, P., Hinton, T., et al. (2011)
730 Development and evaluation of an earth-system Model-HadGEM2. Geoscientific Model
731 Development, 4, 1051-1075. http://dx.doi.org/10.5194/gmd-4-1051-2011

732 Correia I, do Nascimento ER, Gouveia SF (2020) Effects of climate and land-use gradients on avian
733 phylogenetic and functional diversity in a tropical dry forest. Journal of Arid Environments, 173,
734 104024. https://doi.org/10.1016/j.jaridenv.2019.104024

735 Cunha ER, Santos CAG, Silva RM, Bacani VM, Pott A (2021) Future scenarios based on a CA-
736 Markov land use and land cover simulation model for a tropical humid basin in the Cerrado/Atlantic
737 forest ecotone of Brazil. Land Use Policy, 100, 105141.
738 https://doi.org/10.1016/j.landusepol.2020.105141

739 Cunha ER, Santos CAG, Silva RM, Bacani VM, Teodoro PE, Panachuki E, Oliveira NS (2021)
740 Mapping LULC types in the Cerrado-Atlantic Forest ecotone region using a Landsat time series and
741 object-based image approach: A case study of the Prata River Basin, Mato Grosso do Sul, Brazil.
742 Environmental Monitoring and Assessment, 192, 547-567. http://dx.doi.org/10.1007/s10661-020-
743 8093-9

744 da Rocha SJSS, Torres CMME, Villanova PH, Schettini BLS, Jacovine LAG, Leite HG, Gelcer EM,
745 Reis LP, Neves KM, Comini IB, da Silva LF (2020) Drought effects on carbon dynamics of trees in a
746 secondary Atlantic Forest. Forest Ecology and Management, 465, 118097.
747 https://doi.org/10.1016/j.foreco.2020.118097

748 da Silva RM, Montenegro SMGL, Santos CAG (2012) Integration of GIS and remote sensing for
749 estimation of soil loss and prioritization of critical sub-catchments: a case study of Tapacurá
750 catchment. Natural Hazards, 62, 953-970. http://dx.doi.org/10.1007/s11069-012-0128-2

751 Dai C, Qin XS, Lu WT, Huang Y (2020) Assessing adaptation measures on agricultural water
752 productivity under climate change: A case study of Huai River Basin, China. Science of The Total
753 Environment, 721, 137777. https://doi.org/10.1016/j.scitotenv.2020.137777

754 De Andrade CWL, Montenegro SMGL, Montenegro AAA,Lima JRS, Srinivasan R, Jones CA (2019)
755 Soil moisture and discharge modeling in a representative watershed in northeastern Brazil using
756 SWAT. Ecohydrology & Hydrobiology, 19(2), 238-251. https://doi.org/10.1016/j.ecohyd.2018.09.002

757 De Carvalho AL, Menezes RSC, Nóbrega RS, Pinto AS, Ometto JPHB, Randow C, Giarolla A (2015)
758 Impact of climate changes on potential sugarcane yield in Pernambuco, northeastern region of Brazil.
759 Renewable Energy, 78, 26-34. https://doi.org/10.1016/j.renene.2014.12.023

760 de Medeiros IC, da Costa Silva JFCB, Silva RM, Santos CAG (2019) Run-off-erosion modelling and
761 water balance in the Epitácio Pessoa dam river basin, Paraíba State in Brazil. International Journal of
762 Environmental Science and Technology, 16, 3035-3048. http://dx.doi.org/10.1007/s13762-018-1940-3

763 De Oliveira LA, De Miranda JH, Cooke RAC (2018) Water management for sugarcane and corn
764 under future climate scenarios in Brazil. Agricultural Water Management, 201, 199-206.
765 https://doi.org/10.1016/j.agwat.2018.01.019

766 dos Santos JYG (2015) Análise espaço-temporal de processos hidrossedimentológicos na Bacia do Rio
767 Tapacurá. Tese de Doutorado, Universidade Federal de Pernambuco, Recife – PE, 205p.
768 doi:10.13140/RG.2.2.18290.71369.

769 Dos Santos JYG, Silva RM, Carvalho Neto JG, Montenegro SMGL, Santos CAG, Silva AM (2014)
770 Assessment of land-use change on streamflow using GIS, remote sensing and a physically-based
771 model, SWAT, Proc. IAHS, 364, 38–43, doi:10.5194/piahs-364-38-2014.

772 Dos Santos JYG, Silva RM, Carvalho Neto JG, Montenegro SMGL, Santos CAG, Silva AM (2015)
773 Land cover and climate change effects on streamflow and sediment yield: a case study of Tapacurá

774 River basin, Brazil. Proceedings of the International Association of Hydrological Sciences, v. 371, p.
775 189-193. https://doi.org/10.5194/piahs-371-189-2015

776 Eamen L, Brouwer R, Razavi S, (2020) The economic impacts of water supply restrictions due to
777 climate and policy change: a transboundary river basin supply-side input-output analysis. Ecological
778 Economics, 172, 106532. https://doi.org/10.1016/j.ecolecon.2019.106532

779 EMBRAPA – Empresa Brasileira de Agropecuária. (1999) Zoneamento agroecológico do Estado de
780 Pernambuco. Recife: Embrapa Solos UEP Recife/SPRRA-PE.

781 Feron S, Cordero R, Damiani A, Llanillo P. J., Jorquera J, Sepulveda E, Asencio V, Laroze D, Labbe
782 F, Carrasco J, Torres G (2019) Observations and projections of heat waves in South America.
783 Scientific Reports, 9:1–15. https://doi.org/10.1038/s41598-019-44614-4

784 Ferrigo S (2014) Análise de consistência dos parâmetros do modelo SWAT obtidos por calibração
785 automática – estudo de caso na Bacia do Lago Descoberto – DF. PhD. Dissertation, Universidade de
786 Brasília, Brasília – DF, 147p.

787 Fukunaga DC (2012) Estimativa de vazão em bacias hidrográficas do sul do Espírito Santo usando o
788 SWAT. PhD. Dissertation, Universidade Federal do Espírito Santo, Jerônimo Monteiro – ES, 98p.

789 GOOGLE. Google Earth. Google Inc. (2011) Available at: <http://earth.google.com>. Accessed on 14
790 de março de 2019.

791 Gunkel G, Rueter K, Casallas J, Sobral MC (2003) Estudos da limnologia do reservatório de Tapacurá
792 em Pernambuco: problemas da gestão de reservatórios no semi-árido brasileiro. Proceedings XV
793 Símpósio Brasileiro de Recursos Hídricos, Curitiba, Brazil.

794 IBGE – Instituto Brasileiro de Geografia e Estatística (2020) Estimates of the resident population in
795 Brazilian municipalities in 2018. Available at:
796 ftp://ftp.ibge.gov.br/Estimativas_de_Populacao/Estimativas_2020/estimativa_dou_2020.xls. Accessed
797 on 06 September 2020.

798 IPCC – Intergovernmental Panel on Climate Change (2008) Towards new scenarios for analysis of
799 emissions, climate change, impacts, and response strategies. IPCC Expert Meeting Report on New
800 Scenarios, Noordwijkerhout, Intergovernmental Panel on Climate Change.

801 Kusangaya S, Toucher MLW, Garderen EA (2018) valuation of uncertainty in capturing the spatial
802 variability and magnitudes of extreme hydrological events for the uMngeni catchment, South Africa.
803 Journal of Hydrology, 557, 931-946. https://doi.org/10.1016/j.jhydrol.2018.01.017

804 Landis JR, Koch GG (1977) The measurement of observer agreement for categorical data. Biometrics,
805 33(1), 159-174. https://doi.org/10.2307/2529310

806 Lapola DM, Braga DR, Di Giulio GM, Torres RR, Vasconcellos MP (2019) Heat stress vulnerability
807 and risk at the (super) local scale in six Brazilian capitals. Climate Change, 154: 477–492.
808 https://doi.org/10.1007/s10584-019-02459-w

809 Lelis TA, Calijuri ML, Fonseca AS, Lima DC, Rocha EO (2012) Análise de sensibilidade e calibração
810 do modelo SWAT aplicado em Bacia Hidrográfica da Região Sudeste do Brasil. Revista Brasileira de
811 Ciência do Solo, 36: 623-634.

812 Li X, Chen Y (2020) Projecting the future impacts of China's cropland balance policy on ecosystem
813 services under the shared socioeconomic pathways. Journal of Cleaner Production, 250, 119489.
814 https://doi.org/10.1016/j.jclepro.2019.119489

Lillesand TM, Kiefer RW (2000) Remote sensing and digital image interpretation. Wiley, New York, 724 p.

Liu W, Bailey RT, Andersen HE, Jeppesen E, Nielsen A, Peng K, Molina-Navarro E, Park S, Thodsen H, Trolle D (2020) Quantifying the effects of climate change on hydrological regime and stream biota in a groundwater-dominated catchment: A modelling approach combining SWAT-MODFLOW with flow-biota empirical models. Science of The Total Environment, 745, 140933. https://doi.org/10.1016/j.scitotenv.2020.140933

Malutta S (2012) Estudo hidrossedimentológico da Bacia Hidrográfica do Rio Negrinho - SC com o modelo SWAT. PhD. Dissertation, Universidade Federal de Santa Catarina, Florianópolis, 126p.

Marengo JA, Alves LM, Ambrizzi T, Young A, Barreto NJC, Ramos AM (2020) Trends in extreme rainfall and hydrogeometeorological disasters in the Metropolitan Area of São Paulo: a review. Annals of the New York Academy of Sciences. 1472(1): 5-20. https://doi.org/10.1111/nyas.14307

Marin M, Clinciu I, Tudose NC, Ungurean C, Adorjani A, Mihalache AL, Davidescu AA, Davidescu SO, Dinca L, Cacovean H (2020) Assessing the vulnerability of water resources in the context of climate changes in a small forested watershed using SWAT: A review. Environmental Research, 184, 109330. https://doi.org/10.1016/j.envres.2020.109330

McHugh ML (2012) Interrater reliability: The kappa statistic. Biochemia Medica. 22(3): 276–282. https://doi.org/10.11613/bm.2012.031

Melo Neto JO, Silva AM, Mello CR, Méllo Júnior AV (2014) Simulação hidrológica escalar com o modelo SWAT. Revista Brasileira de Recursos Hídricos, 19(1): 177-188.

Montenegro SMGL, Ragab R (2012) Impact of possible climate and land use changes in the semi arid regions: a case study from North Eastern Brazil. Journal of Hydrology, 434-435, 55-68. http://dx.doi.org/10.1016/j.jhydrol.2012.02.036

Moriasi DN, Arnold JG, Van Liew MW, Bingner RL, Harmel RD, Veith TL (2007) Model evaluation guidelines for systematic quantification of accuracy in watershed simulations. Trans. ASABE, 50: 885-900. https://doi.org/10.13031/2013.23153

Nilawar AP, Waikar ML (2019) Impacts of climate change on streamflow and sediment concentration under RCP 4.5 and 8.5: a case study in Purna river basin, India. Science of The Total Environment, 650, Part 2, 2685-2696. https://doi.org/10.1016/j.scitotenv.2018.09.334

Oyama MD, Nobre CA (2004) Climatic consequences of a large-scale desertification in northeast Brazil: a GCM simulation study. Journal of Climate 17: 3203– 3213.

Petelet-Giraud E, Cary L. Cary P, Bertrand G, Giglio-Jacquemot A, Hirata R, Aquilina L, Alves LM, Martins V, Melo AM, Montenegro SMGL, Chatton E, Franzen M, Aurouet A (2017) Multi-layered water resources, management, and uses under the impacts of global changes in a southern coastal metropolis: When will it be already too late? Crossed analysis in Recife, NE Brazil. Science of The Total Environment, 618, 645-657. http://dx.doi.org/10.1016/j.scitotenv.2017.07.228

Pontius Jr RG, Si K (2014) The total operating characteristic to measure diagnostic ability for multiple thresholds. International Journal of Geographical Information Science, 28(3), 570-583. https://doi.org/10.1080/13658816.2013.862623

Ragab R, Bromley J. D'Agostino DR, Lamaddalena N, Trisorio Luizzi G, Dörflinger G, Katsikides S, Montenegro S, Montenegro A (2012) Water Resources Management Under Possible Future Climate and Land Use Changes: The Application of the Integrated Hydrological Modelling System, IHMS. In:

Choukr-Allah R., Ragab R., Rodriguez-Clemente R. (eds) Integrated Water Resources Management in the Mediterranean Region. Springer, Dordrecht. https://doi.org/10.1007/978-94-007-4756-2_5

Ribeiro Neto A, Scott CA, Lima EA, Montenegro SMGL, Cirilo JA (2014) Infrastructure sufficiency in meeting water demand under climate-induced socio-hydrological transition in the urbanizing Capibaribe River basin – Brazil. Hydrology and Earth System Sciences, 18, 3449-3459. http://dx.doi.org/10.5194/hess-18-3449-2014

Rodriguez-Lloveras X, Buytaert W, Benito G (2016) Land use can offset climate change induced increases in erosion in Mediterranean watersheds. Catena, 143, 244-255. https://doi.org/10.1016/j.catena.2016.04.012

Santana, MS, Sampaio EVSB, Giongo V, Menezes RSC, de Jesus KN, de Albuquerque ERGM, do Nascimento DM, Pareyn FGC, Cunha TJF, Sampaio RMB, Primo DC (2019) Carbon and nitrogen stocks of soils under different land uses in Pernambuco state, Brazil. Geoderma Regional, 16, e00205. https://doi.org/10.1016/j.geodrs.2019.e00205

Santos CAG, Brasil Neto RM, Nascimento TVM, Silva RM, Mishra M, Frade TG (2021) Geospatial drought severity analysis based on PERSIANN-CDR-estimated rainfall data for Odisha state in India (1983-2018). Science of The Total Environment, 750, 141258. http://dx.doi.org/10.1016/j.scitotenv.2020.141258

Santos CAG, Nascimento TVM, Silva RM (2020) Analysis of forest cover changes and trends in the Brazilian semiarid region between 2000 and 2018. Environmental Earth Sciences, 18, 10060.

Santos e Silva CM, Silva A, Oliveira P, Lima KC (2013) Dynamical downscaling of the precipitation in Northeast Brazil with a regional climate model during contrasting years. Atmospheric science letters, 15(1): 50-57. https://doi.org/10.1002/asl2.468

Silva LP, Xavier APC, da Silva RM, Santos CAG (2020) Modeling land cover change based on an artificial neural network for a semiarid river basin in northeastern Brazil. Global Ecology and Conservation, 21, e00811. http://dx.doi.org/10.1016/j.gecco.2019.e00811

Silva RM, Dantas JC, Beltrao JA, Santos CAG (2018) Hydrological simulation in a tropical humid basin in the Cerrado biome using the SWAT model. Hydrology Research, 49(3), 908–923. http://dx.doi.org/10.2166/nh.2018.222

Silva RM, Montenegro SMGL, Santos CAG (2012) Integration of GIS and remote sensing for estimation of soil loss and prioritization of critical sub-catchments: a case study of Tapacurá catchment. Natural Hazards, 62, 953-970. http://dx.doi.org/10.1007/s11069-012-0128-2

Silva RM, Santos CAG, Silva AM (2014) Predicting soil erosion and sediment yield in the Tapacurá catchment, Brazil. Journal of Urban and Environmental Engineering, 8(1), 75-82. http://dx.doi.org/10.4090/juee.2014.v8n1.075082

Silva RM, Silva JFCBC, Santos CAG, Silva AM, Brasil Neto RM (2020b) Spatial distribution and estimation of rainfall trends and erosivity in the Epitácio Pessoa reservoir catchment, Paraíba – Brazil. Natural Hazards, 192, p. 765-785. http://dx.doi.org/10.1007/s10661-020-8219-0

Silva RM, Silva LP, Montenegro SMGL, Santos CAG (2010a) Análise da variabilidade espaço-temporal e identificação do padrão da precipitação na bacia do Rio Tapacurá, Pernambuco. Sociedade & Natureza, 22, 357-372. http://dx.doi.org/10.1590/S1982-45132010000200010

Silva RM, Silva LP, Montenegro SMGL, Santos CAG (2010b) Spatial analysis of vegetal cover and sediment yield in Tapacurá river catchment based on remote sensing and GIS. Land Reclamation, 42, 5-16. http://dx.doi.org/10.2478/v10060-008-0059-5

Souza DG, Sfair JC, de Paula AS, Barros MF, Rito KF, Tabarelli M (2019) Multiple drivers of aboveground biomass in a human-modified landscape of the Caatinga dry forest. Forest Ecology and Management, 435, 57-65. https://doi.org/10.1016/j.foreco.2018.12.042

Souza DC, Oyama MD (2011) Climatic consequences of gradual desertification in the semi-arid area of Northeast Brazil. Theoretical and Applied Climatology 103: 345– 357.

Strauch M, Bernhofer C, Koide S, Volk M, Lorz C, Makeschin F (2012) Using precipitation data ensemble for uncertainty analysis in SWAT streamflow simulation. Journal of Hydrology, 414-415: 413-424. https://doi.org/10.1016/j.jhydrol.2011.11.014

Tamm O, Maasikamäe S, Padari A, Tamm T (2018) Modelling the effects of land use and climate change on the water resources in the eastern Baltic Sea region using the SWAT model. Catena, 167, 78-89. https://doi.org/10.1016/j.catena.2018.04.029

Tapiador FJ, Navarro A, Moreno R, Sánchez JL, García-Ortega E (2020) Regional climate models: 30 years of dynamical downscaling. Atmospheric Research, 235, 104785. https://doi.org/10.1016/j.atmosres.2019.104785

Ursulino BS, Montenegro SMGL, Coutinho AP, Coelho VHR, Araújo DCS, Gusmão ACV, Santos Neto SM, Lassabatere L, Angulo-Jaramillo R (2019) Modelling soil water dynamics from soil hydraulic parameters estimated by an alternative method in a tropical experimental basin. Water, 11, 1007-1026. http://dx.doi.org/10.3390/w11051007

Uzeika T, Merten GH, Minella JPG, Moro M (2012) Use of the SWAT model for hydro-sedimentologic simulation in a small rural watershed. Revista Brasileira de Ciências do Solo, 36: 557-565. https://doi.org/10.1590/S0100-06832012000200025

Van Vuuren DP, Edmonds J, Kainuma M, Riahi K, Thomson A, Hibbard K, Hurtt GC, Kram T, Krey V, Lamarque J-F, Masui T, Meinshausen M, Nakicenovic N, Smith SJ, Rose SK (2011) The representative concentration pathways: an overview. Climate Change, 109(5), 415-429. https://doi.org/10.1007/s10584-011-0148-z

Wang Q, Xu Y, Wang Y, Zhang Y, Xiang J, Xu Y, Wang J (2020) Individual and combined impacts of future land-use and climate conditions on extreme hydrological events in a representative basin of the Yangtze River Delta, China. Atmospheric Research, 236, 104805. https://doi.org/10.1016/j.atmosres.2019.104805

Xavier APC, Silva RM (2018) A GIS-based method for temporal dynamic modelling of the land use and land cover in the Tapacurá River basin (PE). Geociências, 31(1), 193-210.

Zhang C, Wang X, Li J, Hua T (2020) Identifying the effect of climate change on desertification in northern China via trend analysis of potential evapotranspiration and precipitation. Ecological Indicators, 112, 106141. https://doi.org/10.1016/j.ecolind.2020.106141

Zhao C, Brissette F, Chen J, Martela J-L (2020) Frequency change of future extreme summer meteorological and hydrological droughts over North America. Journal of Hydrology, 584, 124316. https://doi.org/10.1016/j.jhydrol.2019.124316